Heliyon 9 (2023) e15879

Contents lists available at ScienceDirect

Heliyon

journal homepage: www.cell.com/heliyon

Research article

Connexin 43 dephosphorylation at serine 282 induces spontaneous arrhythmia and increases susceptibility to ischemia/reperfusion injury

Lulin Wu, Tianhui Jiang, Zhiping Fu, Luqi Wang, Hongjie You, Jingyi Xue **, Dali Luo *

Department of Pharmacology, School of Basic Medical Sciences, Beijing Key Laboratory of Metabolic Disturbance Related Cardiovascular Disease, Capital Medical University, Beijing 100069, PR China

ARTICLE INFO

Keywords:
Connexin 43
Arrhythmia
Apoptosis
Ischemia/reperfusion
Phosphorylation

ABSTRACT

Background: Connexin 43 (Cx43), the predominant gap junction protein in hearts, is modified by specific (de)phosphorylation events under physiological and pathological states to affect myocardium function and structure. Previously we found that deficiency in Cx43 S282 phosphorylation could impair intercellular communication and contribute to cardiomyocyte apoptosis by activating p38 mitogen-activated protein kinase (p38 MAPK)/factor-associated suicide (Fas)/Fas-associating protein with a novel death domain (FADD) pathway, which is involved in myocardium injury in ischemia/reperfusion (*I/R*) heart. In addition, mutant at Cx43 S282 substituted with alanine heterozygous mice ($S282A^{+/-}$) exhibited different degrees of ventricular arrhythmias and only some underwent myocardium apoptosis. In this study, we aimed to investigate the role of Cx43 pS282 in different cardiac pathological phenotypes.

Methods: We examined cardiac function, structure, and relevant protein expression in $S282A^{+/-}$ mice (aged 2, 10 and 30 weeks) by electrocardiograph, echocardiography, histological staining, and co-immunoprecipitation followed by Western blot. Intraperitoneal isoprenaline injection and I/R surgery were applied in $S282A^{+/-}$ mice as external stimulus. 2,3,5-triphenyltetrazolium chloride staining was used for myocardium infarction evaluation.

Results: Adult $S282A^{+/-}$ mice (aged 10 and 30 weeks) still exhibited spontaneous arrhythmia. Unlike neonatal stage (aged around 2 weeks), no apoptosis-related manifestations and the activation of p38 MAPK-Fas-FADD apoptotic pathway were observed in adult $S282A^{+/-}$ hearts. $S282A^{+/-}$ neonatal mice with cardiomyocytes apoptosis exhibited more than 60% dephosphorylation at Cx43 S282 than WT mice, while less than 40% S282 dephosphorylation were found in adult $S282A^{+/-}$ mice. In addition, although $S282A^{+/-}$ mice displayed normal cardiac function, they were highly susceptible to isoproterenol-induced ECG alternans and prone to cardiac injury and deaths upon *I/R* attack.

Conclusions: These results reinforce that Cx43 S282 dephosphorylation acts as a susceptibility factor in regulating cardiomyocyte survival and cardiac electrical homeostasis in basal conditions and contributes to myocardium injury in the setting of *I/R*. Cx43 S282 phosphorylation was competent to induce spontaneous arrhythmias, cardiomyocyte apoptosis and deaths based on the degree of S282 dephosphorylation.

* Corresponding author.
** Corresponding author.
E-mail addresses: xuejingyi@ccmu.edu.cn (J. Xue), luodl@ccmu.edu.cn (D. Luo).

https://doi.org/10.1016/j.heliyon.2023.e15879
Received 19 March 2023; Received in revised form 23 April 2023; Accepted 25 April 2023
Available online 1 May 2023

1. Introduction

Gap junctions are transmembrane complexes consisted of connexin proteins that mediate intercellular communication required for several physiological processes including cell synchronization, growth, differentiation and metabolic coordination [1,2]. To date, 20 mouse genes and 21 human genes for connexins have been identified [3]. Connexin 43 (Cx43), as the most abundant connexin isoform expressed in hearts, mediates electrical and metabolic communications between adjacent cardiomyocytes, forming cell-to-cell coupling for electrical propagation responsible for synchronous contraction [1,4–6]. Meanwhile, Cx43 has been recognized as a vital regulator that influences cell cycle progression, migration and apoptosis in cardiomyocytes [7–10]. Loss of Cx43 leads to uncoordinated propagation of electrical impulse and contributes to cardiac arrhythmias [7–10]. Cx43 is phosphoprotein comprised of 21 serine/threonine phosphor-sites, which not only regulates the channel molecular structure and cell-to-cell coupling, but also influences Cx43 life cycle, including synthesis, assembly, traffic and endocytosis [11,12]. Pathological conditions such as ischemia/reperfusion (*I/R*) could affect phosphorylation/dephosphorylation states at different Cx43 serine sites to influence cardiac function and cause cardiac injury, thus can be a target to protect myocardium from injury [13,14].

In previous studies, we identified that Cx43 dephosphorylation at serine 282 could impact cardiac electrical stability and trigger p38 mitogen-activated protein kinase (p38 MAPK), factor-associated suicide (Fas) and Fas-associating protein with a novel death domain (FADD) apoptotic pathway by enhancing physical interaction between Cx43 and p38 MAPK, leading to cardiomyocyte apoptosis. Additionally, the dephosphorylation of S282 and the following activation of apoptosis pathway contributed to cardiac *I/R* injury [15,16]. Further, homozygous mice with Cx43-S282 substituted with alanine (S282A) ceased to develop at the embryonic stage. While approximately 35% heterozygous mice ($S282A^{+/-}$; Het) were normal, the others, around 65%, exhibited abnormal phenotypes, including spontaneous arrhythmias, cardiac dysfunction, and myocardial apoptosis during neonatal stage, and some of them died before maturation [13,15]. It is still unknow about the phenotypes of these alive $S282A^{+/-}$ mice during maturation. Therefore, in this study, we tried to figure out the pathological changes in survived adult mice and the role of Cx43 S282 phosphorylation in it. We found that adult $S282A^{+/-}$ mice did not exhibit myocardium apoptosis and fibrosis, except for spontaneous arrhythmias and the relative Cx43-pS282 level was higher in adult $S282A^{+/-}$ mice than those in infants. With normal cardiac functions, these adult $S282A^{+/-}$ mice were highly susceptible to external stimuli, exhibiting severe arrhythmias and cardiac damage under stimulation of isoproterenol (ISO) or *I/R*. Our study further reinforces the role of Cx43 S282 phosphorylation in cardiomyocyte survival and electrical stability in the heart.

2. Materials and methods

2.1. Animals

Cx43 S282A-mutant mice were obtained and maintained as previously described [13,15]. All animal experiments in this study were approved by the Capital Medical University Animal Care and Use Committee (AEEI-2015-193) and conducted in accordance with the "Guide for the Care and Use of Laboratory Animals" adopted by the Beijing Municipal People's Government.

Survival rates were analyzed among 132 descendants of paired $S282A^{+/-}$ mice parents with constant daily monitoring. Mice were sacrificed as infants (2 weeks old) or as adults (10 and 30 weeks old) to evaluate the cardiac size and weight, histopathological changes, and protein expression.

2.2. Electrocardiograph (ECG) and echocardiography

Surface ECG was used to distinguish mice with arrhythmia from those normal. Surface ECG was monitored with P3 Plus (Data Sciences International) for 5 min after anesthesia with isoflurane. The ECG of each animal was measured at 3 different time points per day. ISO (2 mg/kg) was used as an inducer of arrhythmia by intraperitoneal injection. ECG was recorded for 5 min under anesthesia before ISO injection. A period of 10 min right after ISO injection was chosen to grade arrhythmia scores. Date collected were analyzed using Lab Chart 8 software.

Mice were anesthetized with inhalation of 5% isoflurane (RWB, Batch) and maintained with a 1% concentration of isoflurane in oxygen continuously. 2-dimensional guided M-mode tracings were recorded using a high-resolution ultrasound system (Visual Sonics Vevo 770, Toronto, Canada) equipped with a frequency transducer (frequency band 12–38 MHz). All cardiac function parameters were measured and analyzed using Visual Sonics analysis software (version 2.1.0) from the average of 5 beats.

2.3. Histological analyses

Mouse ventricles were fixed with 4% paraformaldehyde in phosphate-buffered saline. After paraffin embedding, ventricular tissues were sectioned up to 4 μm thickness. H&E, MASSON, and TUNEL staining were carried out in accordance with relevant guidelines as previously described [15].

2.4. Immunoblotting and co-immunoprecipitation

Heart ventricular samples were harvested and lysed in RIPA buffer (Thermo Fisher Scientific, Rockford, IL, USA). After 30 min

gently stirring on ice, samples were centrifuged at 12,000 rpm for 15 min at 4 °C, and the supernatant was collected at once. Protein concentration was determined by BCA assay kit (Thermo Fisher Scientific). Subsequently, the protein samples were subjected to 10% SDS-PAGE and transferred to PVDF membranes. Membranes were blocked in 5% Skim Milk for 1 h at room temperature, and then hybridized with primary antibodies, and probed with Horseradish peroxidase-conjugated secondary antibodies. Immunoblots of protein bands were visualized with immobilon™ western chemiluminescent HPR subtracts (Millipore, Billerica, MA, USA).

Immunoprecipitation was performed as previously described [13,15]. Briefly, protein lysis was incubated with antibody (1 μg/mg proteins; goat *anti*-Cx43, OriGen, Austin, Texas, USA) at 4 °C overnight under constant agitation. Protein A-Sepharose (Thermo Fisher Scientific) was subsequently added to the mixtures and agitation was continued for 4 h at 4 °C. The beads were then washed for 3 times with cold RIPA buffer and proteins were eluted by heating with SDS loading buffer. Western blot was proceeded as described above.

Antibodies used were listed as follows: goat *anti*-Cx43 (OriGen), rabbit *anti*-Cx43 (CST, Danvers, MA, USA), rabbit *anti*-pS282-Cx43 (Biobyt, Cambridge, UK), mouse *anti*-Fas (Santa Cruz), rabbit *anti*-FADD (Santa Cruz, Biotechnology, CA, USA), rabbit *anti*-p-p38 MAPK (CST), rabbit *anti*-p38 MAPKα (CST) and mouse *anti*-GAPDH (ZSGB-BIO, Beijing, China). All were used at the ratio of 1:1000, except for *anti*-Fas and *anti*-FADD antibody at the ratio of 1:500.

2.5. I/R mice model

I/R injury was performed in 10 weeks old WT and S282A$^{+/-}$ mice as previously described [13]. Briefly, mice were anesthetized by intraperitoneal injection of sodium pentobarbital (100 ml/kg). Left anterior descending (LAD) coronary artery was half-tied with an 8-0 silk suture. The mice were subjected to 30 min ligation followed by 2 h reperfusion. Significant S-T elevations detected by ECG was regarded as a sign of successful *I/R* model. Sham mice underwent the same procedures except the ligation of suture beneath the LAD.

2.6. 2,3,5-Triphenyltetrazolium chloride (TTC) staining

TTC staining was used to determine infarct area. Hearts from the sham and *I/R* rats were harvested and then sectioned (thickness, 1 mm) perpendicular to the longitudinal axis. Heart sections were incubated in TTC Staining Solution (1%, Servicebio, China) at 37 °C for 30 min, and then fixed in 4% paraformaldehyde. The images of the sections were captured using FluorChem FC3 (Protein Simple). The infarct area for each section was measured using ImageJ software (National Institutes of Health, Bethesda, MD, USA) by calculating the percentage of ischemia area in the total area.

2.7. Statistical analysis

Statistical analysis was carried out using the SPSS statistics 24.0 software (IBM Corporation, Armonk, NY, USA). Data were presented as mean ± SD and collected from at least three independent experiments. Unpaired two-tailed Student's *t*-test was used to measure difference between two groups, and two-way ANOVA with post Tukey adjustment was used for multiple group comparisons. P

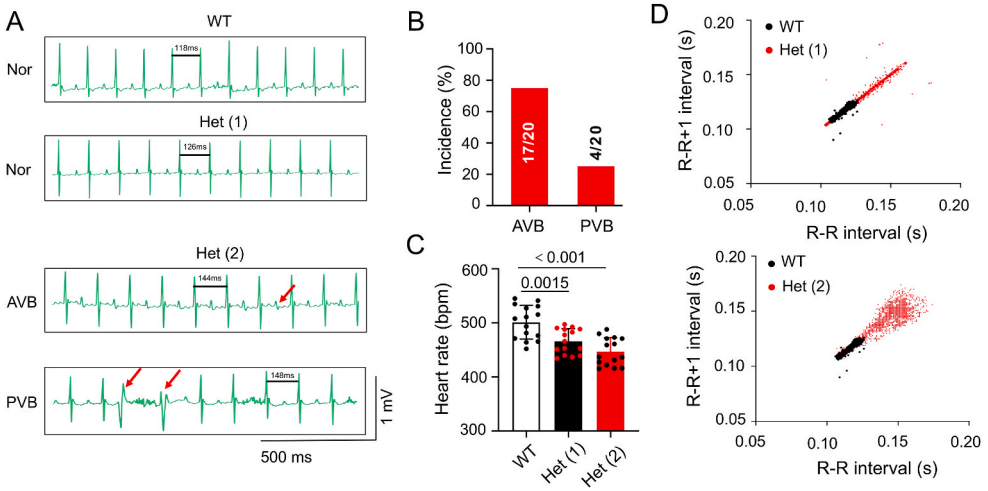

Fig. 1. Adult S282A$^{+/-}$ mice presented with arrhythmia. (A) Different types of ECGs in Het mice at 30 weeks of age; generally normal ECG (Nor), atrioventricular block (AVB) and premature ventricular beat (PVB). Therefore, two groups: Het (1) and Het (2) were divided according to whether arrhythmia occurs. No arrhythmia was identified in WT. Red arrows indicate abnormal beat. (B) Percentages of AVB and PVB were analyzed. (C) Quantification of heart rate in WT and Het mice. The Het mice demonstrated a significant reduction in heart rate. bpm, beats per minute. (D) Poincar'e plots of the R-R intervals show increased heart rate variability in Het mice. Top. WT and Het (1). Bottom. WT and Het (2). Data are expressed as mean ± SD. n values were given in each bar, and P values were obtained as indicated with a line between two groups in each panel using one-way ANOVA test. (For interpretation of the references to colour in this figure legend, the reader is referred to the Web version of this article.)

values less than 0.05 were considered statistically significant.

3. Results

3.1. Adult S282A$^{+/-}$ mice developed spontaneous arrhythmias and are highly susceptible to isoproterenol-induced ECG alternans

In previous studies, pathological changes, including death rates, myocardial apoptosis, myocardial fibrosis, cardiac dysfunction and different types of ventricular arrhythmias were identified in infant S282A$^{+/-}$ mice, and the pathological changes were tightly correlated with cardiac Cx43-pS282 level [13,15]. We raised the mice to 10 weeks and 30 weeks to determine the effect of Cx43 pS282 deficiency in adult mouse hearts. Totally 132 offspring of S282A-mutant mice were used in this study, 32% were wild type (WT), 68% were Het, and no homozygous mice were born from heterozygous crosses. Compared with 100% survival of WT mice, about 30% of the Het mice died between days 7 and 21 after birth, which was in accordance with our previous observations (Supp. Fig. 1) [15]. ~50% adult mice showed spontaneous basal arrhythmias. Mice with generally normal cardiac electrical activity were divided into Het (1) group, while the others presented with arrhythmias, mainly shown as atrioventricular block (AVB) and premature ventricular beats (PVB), were referred as Het (2) (Fig. 1A and B). Meanwhile, both adult Het (1) and Het (2) mice showed significantly decreased heart rate characterized with prolonged R-R interval compared to the WT (Fig. 1C). Dispersed R-R interval between two adjacent QRS wave happened in Het (2), while Het (1) remained slower but regular ventricular beats comparing to WT (Fig. 1D and Supp. Tables S1 and 2).

We further evaluated the cardiac function and structure of adult S282A$^{+/-}$ mice at 10 and 30 weeks of age. M-mode echocardiogram shows no obvious cardiac dysfunction in adult Het mice. The ejection fraction (EF) and fractional shortening (FS) of adult Het mice was slightly lower than WT, but the difference was not statistically significant. Interestingly, the adult Het mice do not have decreased systolic left ventricular wall thickness, which was found in infants Het mice (Supp. Fig. S2) [13,15].

3.2. Adult S282A$^{+/-}$ mice showed decreased heart weight with no morphological change

Infant Het (2) mice have myocardial fibrosis and increased extracellular space [13,15]. To check the heart growth of these mice, we analyzed possible changes in morphology and histology of adult Het mice hearts. As shown in Fig. 2, adult Het (2) mice (aged 10 and 30 weeks) exhibited decreased heart weight proportional to body weight or tibia length (Fig. 2A, B), but with normal morphology and regular myocardium distribution (Fig. 2C, E).

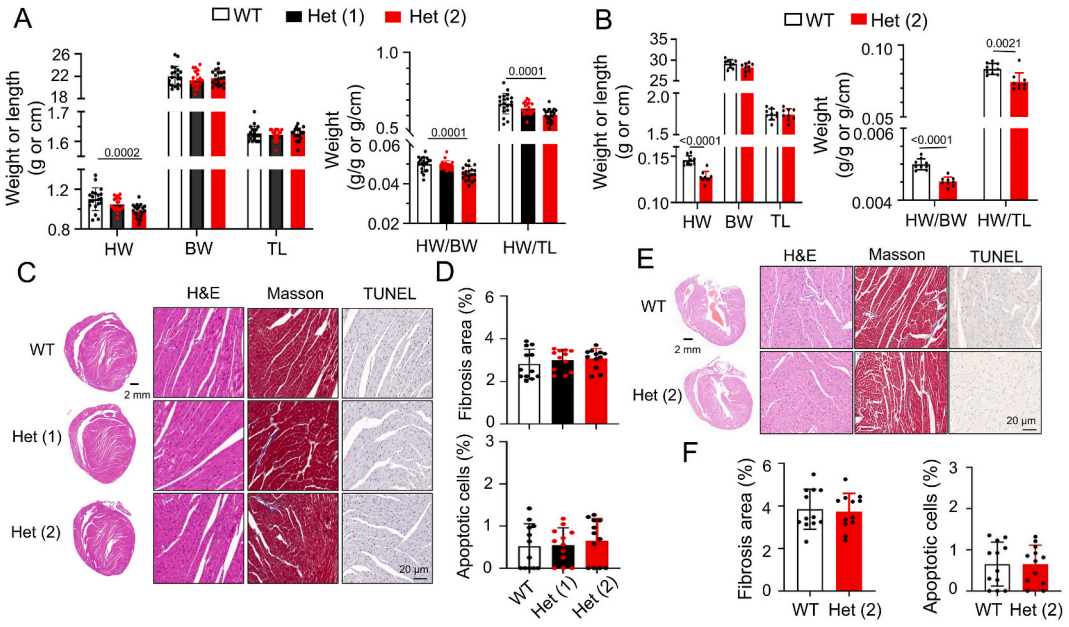

Fig. 2. Adult S282A$^{+/-}$ mice shows no obvious morphological cardiac changes and the sign of apoptosis. (A, B) Comparisons of the heart weight (HW), body weight (BW), tibia length (TL), HW/BW and HW/TL between WT and Het mice at 10 weeks (A) and 30 weeks (B) of age. BW were similar among WT and Het groups, but HW, HW/BW and HW/TL was significantly decreased in adult Het (2) mice, compared with WT. (C, E) Left: Hearts of Het and WT mice at 10 weeks (C) and 30 weeks (E) of age stained with H&E showed no obvious morphological change, the hearts were sectioned longitudinally. Scale bars, 2 mm. Right: Mouse ventricles from mice at 10 weeks (C) and 30 weeks (E) of age were stained with H&E, MASSON or TUNEL as indicated. Nucleus was stained with DAPI. Scale bars, 20 μm. (D, F) Statistical analysis of MASSON staining and TUNEL staining at 10 weeks (D) and 30 weeks (F) of age. Fibrosis area (%) and apoptotic cells (%) were not significantly different between Het and WT. Data are expressed as mean ± SD. n values were given in each bar, and P values were obtained as indicated with a line between two groups in each panel using unpaired two-tailed Student's *t*-test or one-way ANOVA test.

3.3. The difference between adult and neonatal S282A$^{+/-}$ mice in apoptosis phenotype

Previous study has discovered that Cx43 dephosphorylation at S282 could enhance Cx43/p38 MAPK interaction and activate p38 MAPK/Fas/FADD/caspase-8 apoptosis pathway, thus causing myocardium apoptosis in infant Het (2) and Het (3) mice [15]. To confirm whether the apoptosis still exist in adult mice, we performed TUNEL staining on sections of ventricles (Fig. 2C, E). No increase of TUNEL-positive cells was detected in adult Het mice (aged 10 and 30 weeks) (Fig. 2D, F). Western blot analysis of the ventricular samples showed no change in the expression of p-p38, FAS and FADD in both adult Het (1) and Het (2) compared with WT, suggesting that the p38 MAPK/Fas/FAD apoptotic pathway was not activated, and no myocardial apoptosis happened in adult S228A$^{+/-}$ mice (Fig. 3A, B). In contrast, infant mice showed significant increases in p-p38, FAS and FADD expression in Het (2) ventricles (Fig. 3A, B). The pattern of gradually decreased pS282 level from Het (1) to Het (2) mice and Cx43 expression comparing to WT remained unchanged during growth of heterozygous mice [15]. But adult Het (2) mice presented improved relative pS282 level (35% reduction relative to WT-10 weeks old) (37% reduction relative to WT-30 weeks) than those in infants (62% reduction relative to WT-2 weeks) (Fig. 3B).

Then we conducted co-immunoprecipitation approach using a specific antibody for Cx43 to precipitate p-p38, p38 and FADD in ventricles samples from infant and adult S282A$^{+/-}$mice to further investigate changes in apoptotic pathways. The interaction of Cx43 with p-p38 and FADD was significantly increased in the Het (2) ventricles from infant mice compared with WT, but no such change was found in adult Het (2) ventricles (Fig. 3C, D). These results suggested that the Cx43-S282 dephosphorylation in adult Het mice was not enough to trigger the activation of pathological apoptotic process.

3.4. Adult S282A$^{+/-}$ mice were highly susceptible to ISO-induced ECG alternans

Next, we investigated whether S282 dephosphorylation was a susceptibility factor to external pathological stimulus. We performed ECG recordings on S282A$^{+/-}$mice after the injection of ISO, which was used to induce alternans. Notably, the Het (1) mice, which did not display arrhythmias under baseline conditions, exhibited more severe ventricular arrhythmias including ventricular fibrillation and ventricular tachycardia (VT), compared to WT mice upon ISO simulation (Fig. 4A–C).

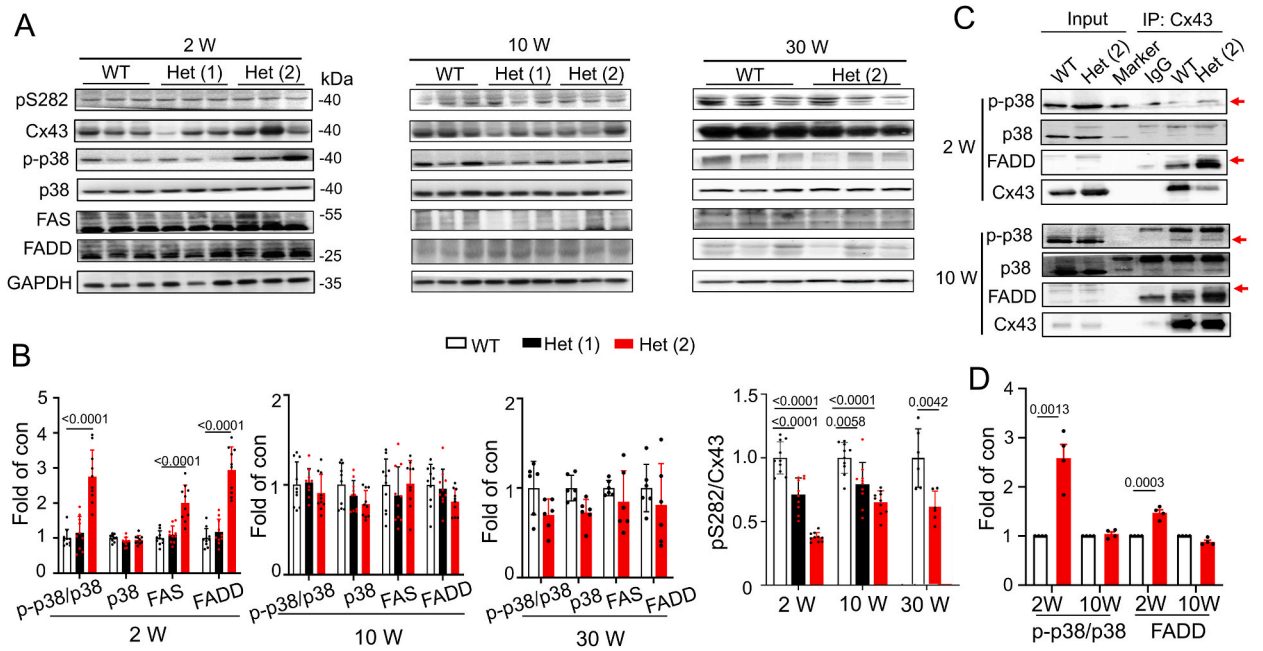

Fig. 3. Adult S282A$^{+/-}$ mice do not exhibit an activation of p38 MAPK/Fas/FADD pathway. (A) Representative Western blots of apoptosis markers (p-p38, p38, Fas, FADD), Cx43 expression and its phosphorylation at S282 from ventricles taken from infants (2W, 2-week-old) and adult (10W, 10-week-old; 30W, 30-week-old) WT and Het mice. GAPDH levels serve as loading control. (B) Quantification of the protein levels shown on Western blot after normalization to GAPDH, p-p38 normalized to p38 MAPK, pS282 normalized to Cx43. The expression of p-p38, Fas and FADD was significantly increased in infants Het (2) mice compared with WT, while there were no obvious changes in the expression of p-p38, Fas and FADD between adult WT and Het mice. (C) Ventricle lysates from infants (2W) and adult (10W) WT and Het (2) mice were immunoprecipitated with *anti*-Cx43 antibody and then Western blotted with *anti*-p-p38, *anti*-p38 or *anti*-FADD antibody. Red arrows indicate the band corresponding to p-p38 and FADD. (D) Quantification of p-p38/p38 and FADD detected in co-immunoprecipitated products. The interaction of Cx43 with p-p38/p38 and FADD was increased in infants Het (2) mice compared with WT, while the interactions were not significantly different between adult WT and Het (2) mice. Data are expressed as mean ± SD. n values were given in each bar, and P values were obtained as indicated with a line between two groups in each panel using unpaired two-tailed Student's *t*-test or one-way ANOVA test. (For interpretation of the references to colour in this figure legend, the reader is referred to the Web version of this article.)

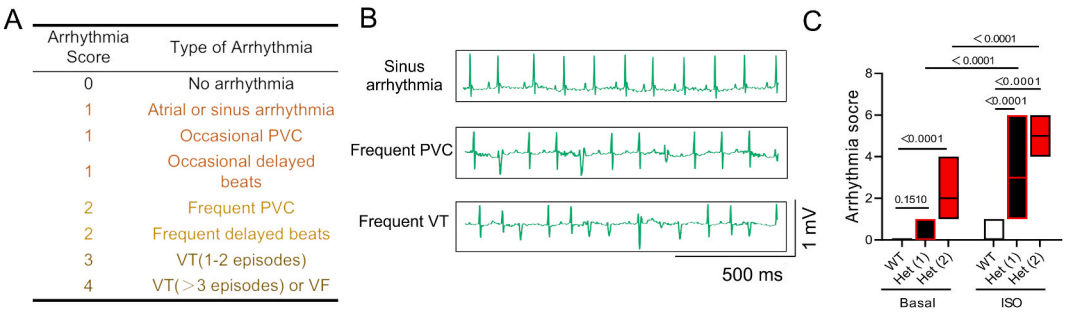

Fig. 4. The arrhythmia susceptibility in S282A$^{+/-}$ mice was increased upon isoproterenol injection. (A) Arrhythmia Score described by Curtis and Walker. (Curtis and Walker, Cardiovasc Res, 1988) (B) The representative typical arrhythmia in 10-week adult Het mice after isoproterenol (ISO) injection. (C) Statistics of the arrhythmia score. The mean of arrhythmia score in Het (2) was higher than that in Het (1) before and after isoproterenol (ISO) injection. WT do not exhibit severe arrhythmia after ISO injection. Data are expressed as min to max with a line at the mean. n = 10. Statistical significance was tested with one-way ANOVA.

3.5. *Adult S282A$^{+/-}$ mice suffered greater damage under I/R attack*

Previously, we found Cx43-pS282 decreased dramatically in *I/R* rats and contributed to the cardiomyocyte apoptosis [13]. We further evaluate the role of Cx43 dephosphorylation under pathological stimulus. WT and Het mice were subjected to surgery of 30 min ligation followed by 2 h reperfusion (LAD, Fig. 5A). A total of 6 WT, 8 Het (1) and 6 Het (2) mice underwent LAD ligation, 2 out of 8 Het (1) and 4 out of 6 Het (2) mice died among reperfusion period, while all WT mice survived after *I/R* injury (Fig. 5B). Histological examination of hearts after *I/R* attack confirmed a significant regional increase in the infarct area through TTC staining analysis in the left ventricular inferior and lateral walls of Het mice compared with those in WT hearts (Fig. 5C and D), indicating that Cx43-S282 dephosphorylation aggravated pathological damage of *I/R* to hearts.

4. Discussion

4.1. *Comparison of adult and infant S282A$^{+/-}$ mice*

We previously found that Cx43 phosphorylation at S282 could mediate electrical stability and cardiomyocyte survival. Deficiency in this residual phosphorylation induces cardiomyocyte apoptosis by triggering p38 MAPK/Fas/FADD pathway in infant Cx43 S282A$^{+/-}$ mice [13,15,17]. Here, in this study we found approximately 70% heterozygous mice grew well to adulthood without

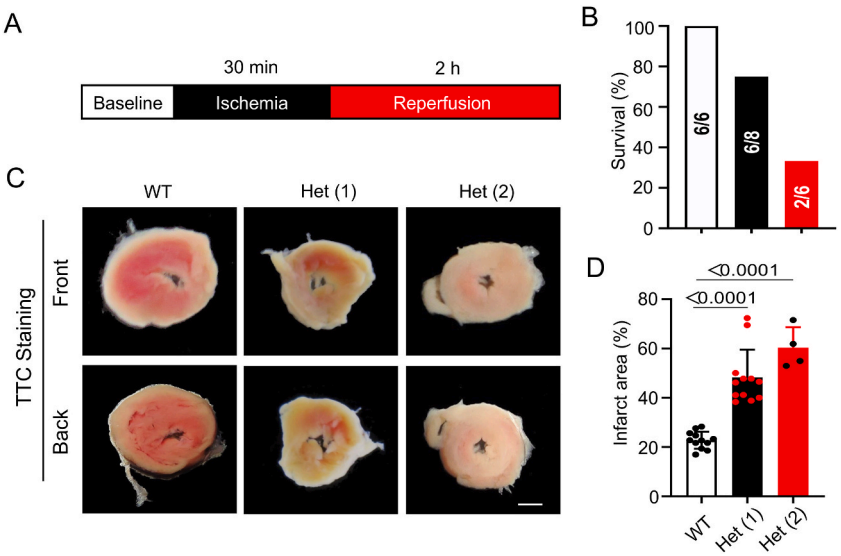

Fig. 5. Ischemia/reperfusion (*I/R*) results in a larger infarct area in S282A$^{+/-}$ mice compared with WT. (A) Schematic representation of the experimental *I/R* protocol used. (B) Survival rate of mice after *I/R*. (C) Representative 2,3,5-triphenyltetrazolium chloride (TTC) staining of heart slices after *I/R*. Scale bars, 2 mm. (D) Infarct area (%) assessed by TTC staining. The infarct area was significantly increased in Het compared with WT. Data are expressed as mean ± SD. n values were given in each bar, and P values were obtained as indicated with a line between two groups in each panel using one-way ANOVA test.

myocardium apoptosis which was found in infant S282A$^{+/-}$ mice (Fig. 1A and 2D, F and Supp.1B). In addition, other pathological changes observed in infants S282A$^{+/-}$ mice, including myocardium fibrosis and cardiac dysfunction [13,15], were not found in adult S282A$^{+/-}$ mice (Fig. 2 and Supp. Fig. S2). Further examinations found that the different phenotypes between adult and infant S282A$^{+/-}$ mice was mainly caused by the different degree of cardiac Cx43-S282 dephosphorylation. Compared with the infants (reduced by ~60%), the level of Cx43-S282 dephosphorylation in adult Het (2) mice was only reduced by ~40%. As a result, it was not sufficient to induce the activation of p38 MAPK/Fas/FADD apoptotic pathway by enhancing interaction between Cx43 and p38 MAPK (Fig. 3), thereby apoptotic response, fibrosis as well as dysfunction disappeared in adult S282A$^{+/-}$ mouse hearts. However, partial recovery of Cx43 S282 phosphorylation due to unknown mechanism of compensation in the adult animals provided us a model to study the effects of graded S282 dephosphorylation, detailed studies are still required to further study the regulatory mechanism of S282 phosphorylation status.

4.2. *Adult S282A$^{+/-}$ mice-different types of arrhythmias*

Although the pathological changes including myocardium apoptosis, myocardium fibrosis and cardiac dysfunction were not shown in adult S282A$^{+/-}$ mice, some adult S282A$^{+/-}$ mice still presented with spontaneous arrhythmias. Combined with previous studies, we found that Het (1) mice with a ~30% reduction in pS282 level did not show arrhythmia. However, further reduced levels of pS282 resulted in a high vulnerability for arrhythmias such as PVB (Fig. 3B) [13,15]. Notably, all S282A$^{+/-}$ mice that presented VT died within 21 days after birth, while approximately 70% mice survived and developed to maturation. In our study, the severity of the arrhythmia does not increase in adult Het (2) mice compared with those in infants, but the incidence of arrhythmia types was different from infants. PVB is the most common type of arrhythmia in infants Het (2) mice, while around 80% adult Het (2) exhibited AVB characterized with prolonged P-R interval, which was not identified in the infants (Fig. 1A, B) [13,15].

The difference of the arrhythmia types between infants and adult Het mice might be due to the ageing-related changes of Cx43 expression in myocardium. As the major connexin in cardiac gap junctions, Cx43 mediates electrical coupling on conduction of action potential in cardiomyocytes that is expressed not only in atria and ventricles, but also in penetrating bundle of the AV junction, which penetrates the fibrous tissue dividing the atria and ventricles and located in the ventricles as the His bundle [18–22]. Studies have showed that both Cx43D378stop mice (deletion of the last five amino acid residues of the Cx43) and Cx43G138R heterozygous mice presented AVB, supporting the possible role of Cx43 in AV conduction [23,24]. Immunofluorescence from the young and old rat cardiac tissues indicate an age-related decrease of Cx43 expression in penetrating bundle, which might impair the AV conduction [20]. S282A$^{+/-}$ mice remain partial function of Cx43, the Cx43 dephosphorylation at S282 might aggravate the impact of Cx43 in AV conduction during ageing, thus caused different arrhythmia types in infants and adult Het (2) mice.

5. Limitations

The mechanisms responsible for partial recovery of Cx43-S282 phosphorylation and the different types of arrhythmias caused by S282 dephosphorylation in adult S282A$^{+/-}$ mice are not clear. In addition, Cx43 S282 phosphorylation might have different effects in different parts of the heart, particularly at AV node, which needs further studies. Meanwhile, it cannot be excluded that the impact of dephosphorylation of Cx43 S282 on other connexons and ion channel proteins, which also regulate conduction of cardiac action potentials.

6. Conclusion

This study demonstrates that the pathological phenotypes and severity occurred in S282A$^{+/-}$ mice are highly dependent on the cardiac Cx43 S282 dephosphorylation level (Supp. Fig. 3). Partial recovery of S282 phosphorylation in adult S282A$^{+/-}$ mice is responsible for the disappearance of the pathological changes including myocardium apoptosis, dysfunction and myocardium fibrosis found in infant S282A$^{+/-}$ heart. Notably, although adult S282A$^{+/-}$ mice do not have basal myocardium apoptosis, they are prone to myocardium infarction and death upon *I/R* attack and intensified ventricular arrhythmias to acute ISO exposure. Therefore, this study reinforced the important physiological and patho-physiological roles of Cx43 S282 phosphorylation in the heart.

Author contribution statement

Lulin Wu: Performed the experiments; Analyzed and interpreted the data; Contributed reagents, materials, analysis tools or data; Wrote the paper. Tianhui Jiang, Zhiping Fu, Luqi Wang, Hongjie You: Analyzed and interpreted the data; Contributed reagents, materials, analysis tools or data. Dali Luo, Jingyi Xue: Conceived and designed the experiments; Analyzed and interpreted the data; Contributed reagents, materials, analysis tools or data; Wrote the paper.

Funding information

Prof. Dali Luo was supported by National Natural Science Foundation of China {82170319, 81570206, 81970197}

Data availability statement

No data was used for the research described in the article.

Declaration of interest's statement

The authors declare no conflict of interest.

Additional information

Supplementary content related to this article has been published online at [URL].

Declaration of competing interest

The authors declare that they have no known competing financial interests or personal relationships that could have appeared to influence the work reported in this paper.

Appendix A. Supplementary data

Supplementary data related to this article can be found at https://doi.org/10.1016/j.heliyon.2023.e15879.

References

[1] M. Kotini, E.H. Barriga, J. Leslie, M. Gentzel, V. Rauschenberger, A. Schambony, R. Mayor, Gap junction protein Connexin-43 is a direct transcriptional regulator of N-cadherin in vivo, Nat. Commun. 9 (1) (2018) 3846.
[2] R.T. Mathias, T.W. White, X. Gong, Lens gap junctions in growth, differentiation, and homeostasis, Physiol. Rev. 90 (1) (2010) 179–206.
[3] G. Söhl, K. Willecke, Gap junctions and the connexin protein family, Cardiovasc. Res. 62 (2004) 228–232.
[4] M.S. Nielsen, L.N. Axelsen, P.L. Sorgen, V. Verma, M. Delmar, N.H. Holstein-Rathlou, Gap junctions, Compr. Physiol. 2 (2012) 1981–2035.
[5] K. Boengler, S. Rainer, Connexins in cardiac ischemia, Curr. Opin. Physiol. 2 (2018) 123–128.
[6] Y. Zhu, Gap junction-dependent and -independent functions of Connexin43 in biology, Biology 11 (2) (2022) 283.
[7] F. Rinaldi, E.M. Hartfield, L.A. Crompton, J.L. Badger, C.P. Glover, C.M. Kelly, et al., Cross-regulation of Connexin43 and β-catenin influences differentiation of human neural progenitor cells, Cell Death Dis. 5 (1) (2014) e1017.
[8] E. Leithe, M. Mesnil, T. Aasen, The connexin 43 C-terminus: a tail of many tales, Biochim. Biophys. Acta Biomembr. 1860 (2018) 48–64.
[9] C. Cina, K. Maass, M. Theis, K. Willecke, J.F. Bechberger, C.C. Naus, Involvement of the cytoplasmic C-terminal domain of connexin43 in neuronal migration, J. Neurosci. 29 (2009) 2009–2021.
[10] L. Matsuuchi, C.C. Naus, Gap junction proteins on the move: connexins, the cytoskeleton and migration, Biochim. Biophys. Acta 1828 (2013) 94–108.
[11] A. Rodríguez-Sinovas, J.A. Sánchez, L. Valls-Lacalle, M. Consegal, I. Ferreira-González, Connexins in the heart: regulation, function and involvement in cardiac disease, Int. J. Mol. Sci. 22 (2021) 4413.
[12] Z.P. Fu, L.L. Wu, J.Y. Xue, L.E. Zhang, C. Li, H.J. You, et al., Connexin 43 hyper-phosphorylation at serine 282 triggers apoptosis in rat cardiomyocytes via activation of mitochondrial apoptotic pathway, Acta Pharmacol. Sin. 43 (8) (2022) 1970–1978.
[13] J. Xue, X. Yan, Y. Yang, M. Chen, L. Wu, Z. Gou, et al., Connexin 43 dephosphorylation contributes to arrhythmias and cardiomyocyte apoptosis in ischemia/reperfusion hearts, Basic Res. Cardiol. 114 (5) (2019) 40.
[14] B.F. Remo, J. Qu, F.M. Volpicelli, S. Giovannone, D. Shin, J. Lader, et al., Phosphatase-resistant gap junctions inhibit pathological remodeling and prevent arrhythmias, Circ. Res. 108 (2011) 1459–1466.
[15] Y. Yang, X. Yan, J. Xue, Y. Zheng, M. Chen, Z. Sun, et al., Connexin43 dephosphorylation at serine 282 is associated with connexin43-mediated cardiomyocyte apoptosis, Cell Death Differ. 26 (2019) 1332–1345.
[16] Z. Sun, Y. Yang, L. Wu, S. Talabieke, H. You, Y. Zheng, et al., Connexin 43-serine 282 modulates serine 279 phosphorylation in cardiomyocytes, Biochem. Biophys. Res. Commun. 513 (2019) 567–572.
[17] M. Kang, N. Lin, C. Li, Q. Meng, Y. Zheng, X. Yan, et al., Cx43 phosphorylation on S279/282 and intercellular communication are regulated by IP3/IP3 receptor signaling, Cell Commun. Signal. 12 (2014) 58.
[18] V.P. Nikolski, S.A. Jones, M.K. Lancaster, M.R. Boyett, I.R. Efimov, Cx43 and dual-pathway electrophysiology of the atrioventricular node and atrioventricular nodal reentry, Circ. Res. 92 (2003) 469–475.
[19] M.R. Boyett, S. Inada, S. Yoo, J. Li, J. Liu, J. Tellez, et al., Connexins in the sinoatrial and atrioventricular nodes, Adv. Cardiol. 42 (2006) 175–197.
[20] Y. Saeed, I.P. Temple, Z. Borbas, A. Atkinson, J. Yanni, Maczewski Met al, Structural and functional remodeling of the atrioventricular node with aging in rats: the role of hyperpolarization-activated cyclic nucleotide-gated and ryanodine 2 channels, Heart Rhythm 15 (2018) 752–760.
[21] J.Á. Cabrera, R.H. Anderson, A. Porta-Sánchez, Y. Macías, Ó. Cano, D.E. Spicer, D. Sánchez-Quintana, The atrioventricular conduction Axis and its implications for permanent pacing, Arrhythmia Electrophysiol. Rev. 10 (2021) 181–189.
[22] I.P. Temple, S. Inada, H. Dobrzynski, M.R. Boyett, Connexins and the atrioventricular node, Heart Rhythm 10 (2013) 297–304.
[23] I. Lübkemeier, R.P. Requardt, X. Lin, P. Sasse, R. Andrié, J.W. Schrickel, et al., Deletion of the last five C-terminal amino acid residues of connexin43 leads to lethal ventricular arrhythmias in mice without affecting coupling via gap junction channels, Basic Res. Cardiol. 108 (2013) 348.
[24] R. Dobrowolski, P. Sasse, J.W. Schrickel, M. Watkins, J.S. Kim, M. Rackauskas, et al., The conditional connexin43G138R mouse mutant represents a new model of hereditary oculodentodigital dysplasia in humans, Hum. Mol. Genet. 17 (2008) 539–554.